Article

TRANSPARENT PROCESS OPEN ACCESS

THE EMBO JOURNAL

BRD4 directs hematopoietic stem cell development and modulates macrophage inflammatory responses

Anup Dey[1,§], Wenjing Yang[2,§], Anne Gegonne[3,§], Akira Nishiyama[1,†,§], Richard Pan[1,§], Ryoji Yagi[4,¶,§], Alex Grinberg[1,§], Fred D Finkelman[5], Karl Pfeifer[1,§], Jinfang Zhu[4,§], Dinah Singer[3,§], Jun Zhu[2,§] & Keiko Ozato[1,*,§]

Abstract

BRD4 is a BET family protein that binds acetylated histones and regulates transcription. BET/BRD4 inhibitors block blood cancer growth and inflammation and serve as a new therapeutic strategy. However, the biological role of BRD4 in normal hematopoiesis and inflammation is not fully understood. Analysis of Brd4 conditional knockout (KO) mice showed that BRD4 is required for hematopoietic stem cell expansion and progenitor development. Nevertheless, BRD4 played limited roles in macrophage development and inflammatory response to LPS. ChIP-seq analysis showed that despite its limited importance, BRD4 broadly occupied the macrophage genome and participated in super-enhancer (SE) formation. Although BRD4 is critical for SE formation in cancer, BRD4 was not required for macrophage SEs, as KO macrophages created alternate, BRD4-less SEs that compensated BRD4 loss. This and additional mechanisms led to the retention of inflammatory responses in macrophages. Our results illustrate a context-dependent role of BRD4 and plasticity of epigenetic regulation.

Keywords BRD4; hematopoietic stem cells; LPS; macrophages; super-enhancers
Subject Categories Immunology; Stem Cells; Transcription
DOI 10.15252/embj.2018100293 | Received 18 July 2018 | Revised 28 January 2019 | Accepted 29 January 2019 | Published online 6 March 2019
The EMBO Journal (2019) 38: e100293

Introduction

BRD4 is a double bromodomain protein of the BET family, expressed ubiquitously at high levels (Dey *et al*, 2000; Wu & Ghosh, 2003). BRD4 broadly occupies various regions of the genome by binding to acetylated histones (Dey *et al*, 2003, 2009; Nishiyama *et al*, 2006; Zhang *et al*, 2012; Hnisz *et al*, 2013; Lovén *et al*, 2013; Kanno *et al*, 2014). BRD4 is also a prominent component of super-enhancers (SEs) in normal and cancer cells and helps define cell type and lineage specificity (Hnisz *et al*, 2013; Lovén *et al*, 2013; Whyte Warren *et al*, 2013; Pelish *et al*, 2015). SEs are large regulatory DNAs, enriched with RNA polymerase II (PoI II) and acetylated H3 at K27 (H3K27ac) (Hnisz *et al*, 2013). BRD4 also binds to genic regions, most strongly at/near the transcription start site (TSS), thereby facilitating transcription elongation (Jang *et al*, 2005; Yang *et al*, 2005; Kanno *et al*, 2014). BRD4 employs other mechanisms to promote transcription, including its kinase activity (Devaiah *et al*, 2016; Winter *et al*, 2017).

Recent development of small molecule inhibitors selective for the BET family greatly advanced BRD4 research, including its role in cancers and inflammatory diseases (Filippakopoulos *et al*, 2010; Nicodeme *et al*, 2010). These inhibitors potently inhibit growth of various cancers, particularly blood cancers, including leukemia, lymphoma, and myeloma (Zuber *et al*, 2011; Lovén *et al*, 2013; Ceribelli *et al*, 2014; Pelish *et al*, 2015; Bhagwat Anand *et al*, 2016). Some of these studies showed that the inhibitors disrupt BRD4-bound SEs, resulting in oncogene downregulation (Lovén *et al*, 2013; Pelish *et al*, 2015; Bhagwat Anand *et al*, 2016). These findings offered a possible mechanism of inhibitor action. These drugs also inhibit inflammation and ameliorate related diseases, including LPS-induced sepsis, EAE-based neuroinflammation, diabetes, and cardiovascular diseases (Nicodeme *et al*, 2010; Bandukwala *et al*, 2012; Anand *et al*, 2013; Belkina *et al*, 2013; Mele *et al*, 2013; Brown Jonathan *et al*, 2014; Fu *et al*, 2014; Duan *et al*, 2017). With these encouraging effects, BET inhibitors offer new therapeutic possibilities, mainly for blood cancers and inflammation (Belkina & Denis, 2012; Ceribelli *et al*, 2014; Berthon *et al*, 2016; Ghosh *et al*, 2017).

1 Division of Developmental Biology, National Institute of Child Health and Human Development, Bethesda, MD, USA
2 The DNA Sequencing and Computational Biology, National Heart, Lung and Blood Institute, Bethesda, MD, USA
3 Experimental Immunology Branch, National Cancer Institute, Bethesda, MD, USA
4 Laboratory of Immunology, National Institute of Allergy and Infectious Diseases, National Institutes of Health, Bethesda, MD, USA
5 Department of Pediatrics, Cincinnati Children's Hospital, Cincinnati, OH, USA
*Corresponding author. Tel: +1 301496 9184; E-mail: ozatok@nih.gov
†Present address: Department of Immunology, Graduate School of Medicine, Yokohama City University, Yokohama, Japan
¶Present address: Department of Immunology, Graduate School of Medicine, Chiba University, Chiba, Japan

A potential problem using these drugs in therapy, however, is that their effects on normal cells are not fully evaluated (Andrieu *et al*, 2016). Particularly problematic is the dearth of knowledge on the role of BRD4 in hematopoietic cells, in that although BRD4 is essential for early embryogenesis in mice, its role in the development and function of hematopoietic cells has remained elusive. It is unknown whether and to what extent BRD4 is required for hematopoiesis and inflammatory responses.

Here, we show that BRD4 is indispensable for the development and function of HSCs, but dispensable for macrophage inflammation to a significant extent. ChIP-seq analysis revealed that BRD4 broadly occupies genic regions and SEs in quiescent macrophages. Further, LPS stimulation dramatically altered BRD4 distribution patterns. We demonstrate that Brd4KO macrophages retain SEs by forming alternative regulatory network. Lastly, we show that NF-κB binding was elevated in Brd4 KO macrophages, which may provide a compensatory mechanism to retain inflammatory responses. Together, our work highlights a context-dependent role of BRD4 and offers additional clues to therapeutic use of BET inhibitors.

Results

Vav-Cre-based Brd4 deletion blocks hematopoietic stem cell development

To construct Brd4 conditional knockout (KO) mice, the endogenous Brd4 locus was replaced, by homologous recombination, with a vector containing loxP sites flanking Brd4 exon 3 (Fig 1A). Brd4 $^{fl/fl}$ mice were crossed with those carrying Vav-Cre, LysM-Cre, or ER^{T2}-Cre to generate cell-type-specific Brd4 KO mice. Examples of successful Brd4 deletion by ER^{T2}-Cre (Fig 1B and see also Appendix Fig S1A) and depletion of Brd4 mRNA and the protein are shown in Fig 1C. To study the role of BRD4 in early hematopoiesis, we tested Brd4 $^{fl/fl}$ Vav-Cre mice (Georgiades *et al*, 2002). qRT–PCR and immunoblot experiments confirmed thorough depletion of BRD4 in resultant cells (Fig 1D). Strikingly, the number of Brd4 KO offspring obtained from multiple crosses was far fewer than expected (3 out of 204, Appendix Fig S1B). Majority of KO embryos died at birth, presumably due to defective blood supply. Brd4KO embryos were readily distinguished from wild-type (WT) embryos (Brd4 $^{fl/fl}$ and/or Brd4$^{+/+}$, Vav-Cre) by a reduced size and pale hue of fetal liver (Fig 1E). Flow cytometry analysis of fetal liver cells showed a marked reduction of Lin$^-$ Sca$^+$cKit$^+$ (LSK) population in KO embryos (Fig 1F, left). Further analysis of LSK population found a severe reduction in Flt3^{lo} and Flt3^{hI} cells, which represent hematopoietic stem cells (HSCs) and multipotent progenitor (MPP) cells, respectively (a diagram in Fig 1G; Adolfsson *et al*, 2005). Accordingly, total number of LSK cells, HSCs, and MPPs were strikingly lower in KO embryos relative to WT, pointing to the lack of HSC proliferation in KO mice (Fig 1F, right panels). Consequently, cells with myeloid and lymphoid cell markers (GR-1 or B220 vs. CD11b) were likewise greatly reduced in KO embryos (Fig 1H). Additionally, we examined two adult Brd4 KO mice that escaped fetal death for the presence of myeloid or lymphoid lineage cells (Fig EV1A and B). Cells carrying markers for these lineages were drastically reduced in KO bone marrow and spleen, indicating that Brd4 KO mice are largely devoid of functional immune cells. Together, BRD4 is critically required for the generation of embryonic HSCs and subsequent progenitor development.

LysM-Cre-based Brd4 deletion compromises development and proliferation of resident peritoneal macrophages

We sought to study the role of Brd4 in macrophages, because they are a primary source of inflammation. Resident macrophages originate from yolk-sac progenitors, while circulating macrophages are derived from bone marrow HSCs Using Brd4 $^{fl/fl}$ LysM-Cre mice (Appendix Fig S2A), we first examined the effect of Brd4 deletion in peritoneal macrophages, representative resident macrophages. First, total peritoneal cavity cells were stained with CD19-FITC, CD11b-PE, and F4/80-APC to depict compensation controls (Appendix Fig S2B). Data in Fig 2A showed that CD19$^-$ F4/80$^+$ macrophages were fewer in KO peritoneum than WT counterpart. Brd4 KO macrophages were constituted with large numbers of F4/80^{low} and CD11b^{low} population, whereas WT macrophages were predominantly F4/80^{high,} CD11b^{high} (Fig 2A, middle panel; Ghosn *et al*, 2010). These results indicate that Brd4 deletion compromises development of resident

Figure 1. Vav-Cre deletion of Brd4 blocks HSC development.

A A schematic representation of targeted deletion of mouse Brd4. The exon–intron organization of the Brd4 locus (top). Targeting vector contained exon 3 flanked by LoxP sites (green) and a neomycin resistance gene flanked by FRT (white). Cre-mediated recombination should cause deletion of exon 3 resulting in loss of BRD4 expression (bottom).

B Genotyping of Brd4 $^{fl/fl}$ mice with ER^{T2}-Cre (Cre) or without ER^{T2} -Cre (+/+). Tamoxifen treatment deleted 2.2 kb Brd4 $^{fl/fl}$ fragment from Cre/+ and Cre/Cre mice (top). Cre/+, Cre/Cre and +/+ mice were confirmed by the presence of ER^{T2} -Cre band (Cre) or its absence (WT) (bottom).

C WT and Brd4 KO cells were tested for mRNA (left) and the protein (right) by qRT–PCR and immunoblot assays. Values represent the average of three experiments ± SD.

D Vav-Cre-mediated Brd4 depletion was verified for cells from Brd4 $^{fl/fl}$ Vav-Cre mice (fetal liver or spleen) by qRT–PCR and immunoblot (left and right). Values represent the average of three experiments ± SD.

E Photographic images of E14.5 embryos from WT and KO mice.

F Corresponding flow cytometric profile of Lin$^-$ fetal liver cells stained with cKit and Sca-1 antibodies examining early hematopoietic progenitor population (LSK) (left). LSK populations were further divided by the Flt3 marker to detect HSCs and MPPs (middle). The number of total cells, e.g., LSKs, HSCs, MPPs, in a fetal liver was estimated on indicated days of embryonic development (E13.5, E14.5, and E17.5). Values are the average of 3–5 embryos ± SD (right).

G A schematic of hematopoietic stem cell and early progenitor cell pathways.

H Representative flow cytometric profile of CD71$^-$ cells stained for the myeloid and lymphoid markers. Values are the average of 3 E17.5 embryos ± SD.

Data information: Statistical significance in all figures was determined by two-tailed unpaired *t*-test and is indicated by: *$P < 0.05$, **$P < 0.01$, ***$P < 0.001$, NS: no significance.

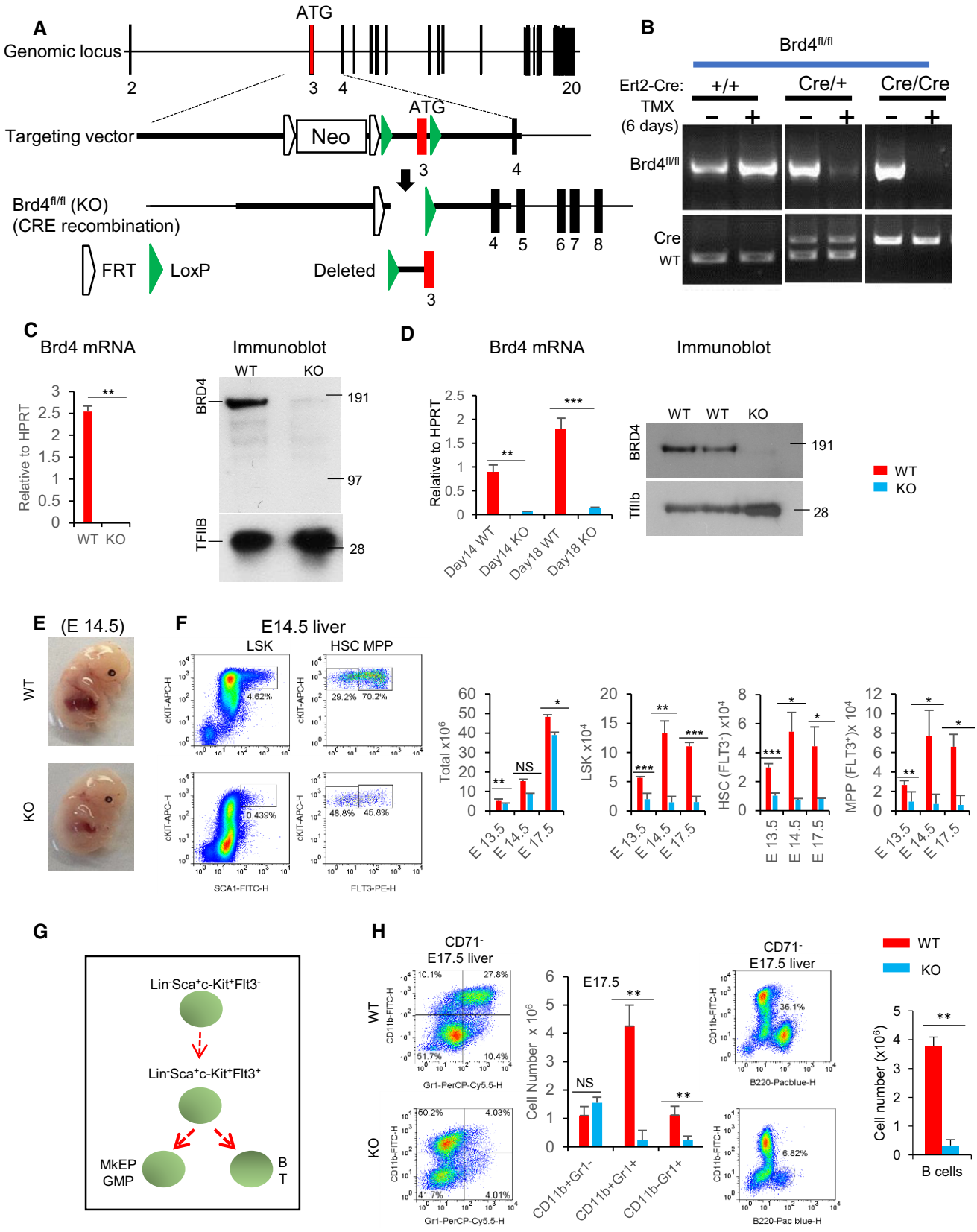
A
Genomic locus
ATG
2
3
4
20
Targeting vector
Neo
Brd4fl/fl (KO)
(CRE recombination)
FRT
LoxP
Deleted
B
Brd4fl/fl
Ert2-Cre:
TMX
(6 days)
+/+
Cre/+
Cre/Cre
Brd4fl/fl
Cre
WT
C
Brd4 mRNA
Immunoblot
Relative to HPRT
WT KO
BRD4
TFIIB
191
97
28
D
Brd4 mRNA
Immunoblot
Relative to HPRT
Day14 WT
Day14 KO
Day18 WT
Day18 KO
WT WT KO
BRD4
TfIIb
191
28
WT
KO
E
(E 14.5)
WT
KO
F
E14.5 liver
LSK
HSC MPP
cKIT-APC-H
SCA1-FITC-H
FLT3-PE-H
4.62%
29.2%
70.2%
0.439%
48.8%
45.8%
Total x10^6
LSK x10^4
HSC (FLT3-) x10^4
MPP (FLT3+)x 10^4
NS
E 13.5
E 14.5
E 17.5
G
Lin-Sca+c-Kit+Flt3-
Lin-Sca+c-Kit+Flt3+
MkEP
GMP
B
T
H
CD71-
E17.5 liver
WT
KO
CD11b-FITC-H
Gr1-PerCP-Cy5.5-H
10.1%
27.8%
51.7%
10.4%
50.2%
4.03%
41.7%
4.01%
E17.5
Cell Number x 10^6
CD11b+Gr1-
CD11b+Gr1+
CD11b-Gr1+
B220-Pacblue-H
B220-Pac blue-H
36.1%
6.82%
WT
KO
Cell number (x10^6)
B cells

Figure 1.

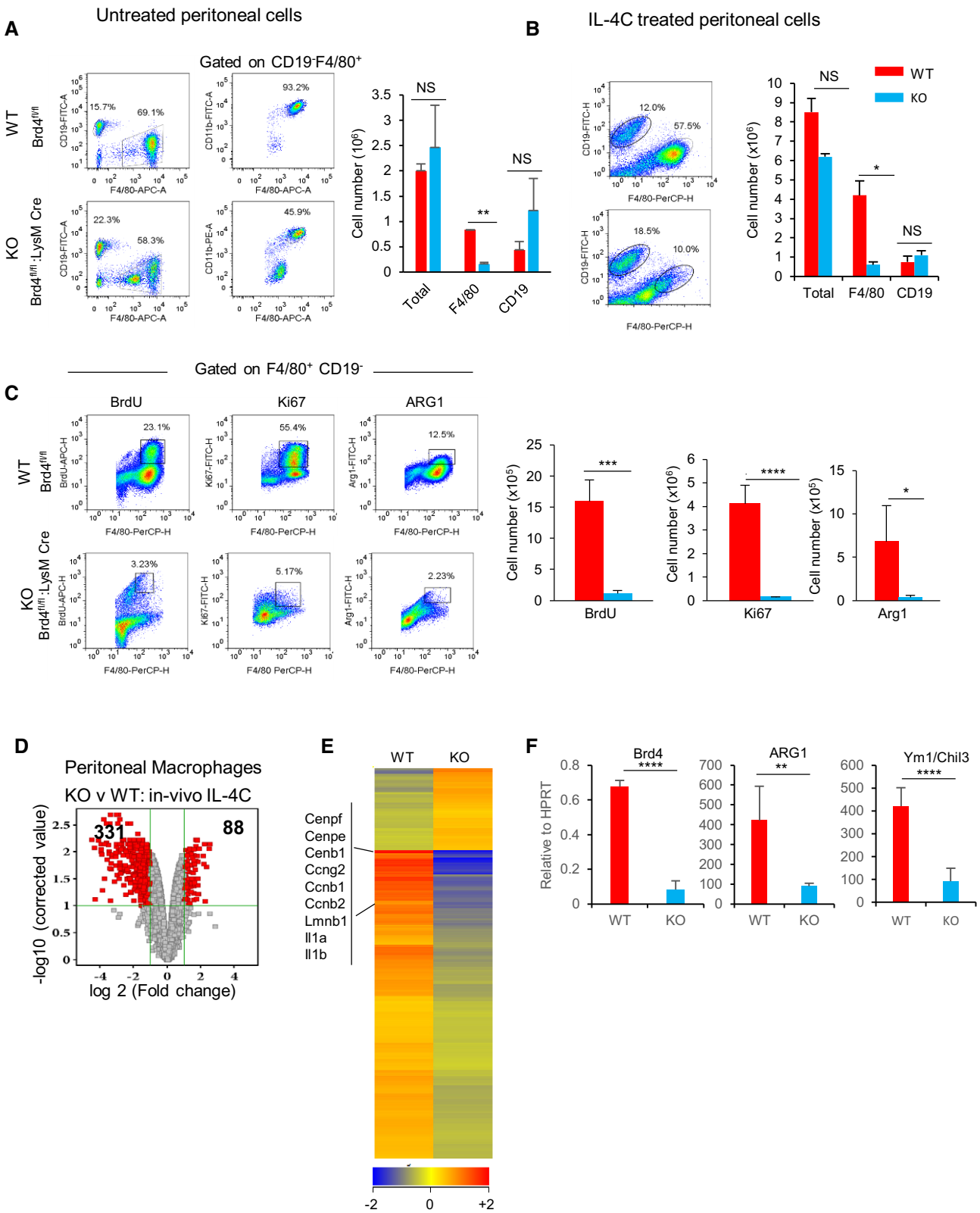

Figure 2.

Figure 2. LysM-Cre deletion of Brd4 impairs development and proliferation of resident peritoneal macrophages.

A Flow cytometry profiles of peritoneal cells from WT and KO mice stained for CD19 and F4/80 (left). FACS profile of $CD19^-$ subset showing $CD11b^+$ and $F4/80^+$ subsets of cells from WT and KO macrophage populations (middle). Cell numbers (right) represent the average of four WT and four Brd4 KO mice ± SD. Note a reduction in $F4/80^+$ cells from Brd4 KO peritoneum.

B Flow cytometry profiles of peritoneal cells from IL-4C-injected WT and KO mice (left). Cell numbers (right) represent the average of four WT and four Brd4 KO mice ± SD.

C Flow cytometry profiles of BrdU incorporation, Ki-67, and ARG1 expression in peritoneal cells (gated for $F4/80^+$ and $CD19^-$ macrophages) from IL-4C-treated WT and KO mice (left). The numbers of cells positive for BrdU, Ki-67, and ARG1 (right). The numbers represent the average of three experiments ± SD.

D Microarray analysis of macrophage gene expression in IL-4C-treated WT or Brd4 KO mice. Macrophages were isolated from peritoneal cells by the MACS system. Differentially expressed genes were identified with a cutoff line of log2 fold change > 2 difference with *P*-value of < 0.05. Red dots indicate differentially expressed genes (KO vs. WT), and gray dots are those below the cutoff line.

E Hierarchical clustering of differentially expressed genes. Representative downregulated genes in KO macrophages are shown by gene symbols. See GO analysis in Appendix Fig S2C.

F qRT–PCR confirmation of representative genes downregulated in KO macrophages from IL-4C-treated mice. Values represent the average of three independent experiments ± SD.

Data information: Statistical significance in all figures was determined by two-tailed unpaired *t*-test and is indicated by: $*P < 0.05$, $**P < 0.01$, $***P < 0.001$, $****P < 0.0001$, NS: no significance.

peritoneal macrophages, although it does not totally abolish the process. Peritoneal macrophages respond to the Th2 cytokine IL-4 and undergo proliferation (Jenkins *et al*, 2011, 2013). IL-4 stimulation, however, does not cause macrophage recruitment from elsewhere in the body. To test whether BRD4 regulates macrophage proliferation, we injected IL-4C complexes into KO and WT mice and examined macrophage proliferation (Jenkins *et al*, 2013). Results in Fig 2B showed a large increase in macrophage numbers in WT mice, but not in Brd4 KO mice, indicative of defective proliferation (compare $F4/80^+$ cell population in Fig 2A and B, right panels). Analysis of BrdU incorporation, Ki-67, and ARG1 expression confirmed reduced cell division in Brd4 KO macrophages (Fig 2C). Thus, resident macrophages require BRD4 for full differentiation and IL-4-induced proliferation. Microarray analyses of peritoneal macrophages from IL-4C-treated mice showed that genes involved in cell division were downregulated in KO macrophages (Fig 2D and E). Hierarchical clustering and GO analysis of downregulated genes revealed marked enrichment in categories related to cell division and mitosis (Fig 2E and Appendix Fig S2C). In addition, M2-specific genes, such as *Arg1* and *Chil3/Ym1*, were downregulated in KO macrophages, some of which were verified by qRT–PCR (Fig 2F). As a comparison, microarray analysis was also performed for peritoneal macrophages treated with IL-4 *ex vivo* (Fig EV2A–C). The *ex vivo* treatment did not induce proliferation in either WT or KO macrophages, as anticipated. Nevertheless, 30-40% of differentially expressed genes were shared by *in vivo* and *ex vivo* IL-4-treated macrophages (Fig EV2D and E). These results show that Brd4 deletion obliterates macrophage's ability to proliferate, while retaining many macrophage-specific traits. Similarly, Brd4 deletion partially impaired typical M1 responses upon IFN-γ stimulation (Fig EV2F).

Brd4 deletion partially inhibits LPS-induced gene expression in BM-derived macrophages

BET inhibitors have been extensively tested in BM-derived macrophages, particularly in the context of LPS-induced inflammation (Nicodeme *et al*, 2010; Belkina *et al*, 2013; Brown Jonathan *et al*, 2014). We thus examined the effect of Brd4 deletion on BM-derived macrophages in detail, using ER^{T2}-Cre (Fig 3A for experimental diagram and confirmation of Brd4 deletion in Fig 1B and C). $CD11b^+F4/80^+$ macrophages were generated comparably from WT and KO cultures, showing similar total yields and FACS profiles (Fig 3B). Virtually identical results were observed with BM macrophages generated by LysM-Cre (Fig EV3A). These results led us to conclude that Brd4 deletion does not grossly alter the course of BM macrophage development. LPS is a powerful inflammatory signal, relevant to chronic diseases. It has been shown that knockdown of individual BET proteins or treatment with BET inhibitors decreases expression of certain LPS-induced genes in BM macrophages (Nicodeme *et al*, 2010; Belkina *et al*, 2013; Brown Jonathan *et al*, 2014). To determine the role of BRD4 more definitively, we performed RNA-seq analysis for BM macrophages stimulated by LPS for 4 h. We defined differentially expressed genes as those with > 2 fold change with a significance threshold set at FDR < 0.1 following the DESeq2 program (Robinson *et al*, 2009). Since BRD4 broadly affects transcription, we assessed whether Brd4 disruption changes global gene expression. We plotted linear regression for LPS-induced genes with RPKM values (log2 LPS/UT ≥ 1) in Brd4 KO and WT cells (Appendix Fig S3A). Results showed that the two conditions are well correlated (slope = 0.987). Given the modest intercept, the global effect of Brd4 KO is likely to be low. MA plots in Fig 3C (left and middle panels) show that more genes were downregulated than upregulated in KO macrophages compared to WT cells both under untreated (UT) conditions and after LPS stimulation. More importantly, LPS treatment induced 868 genes in WT cells (Venn diagram in Fig 3D). Of them, 206 genes were downregulated in Brd4 KO macrophages, whereas 12 genes were upregulated in KO macrophages. qRT–PCR analysis of independently prepared samples confirmed the RNA-seq data, including *Tnf, Il1b* (genes unaffected in KO), *Ptgs2, Fcgr2b, Il6* (downregulated by KO), and *Ccl2* and *Ccl7* (upregulated by KO) (Fig 3E). Together, only ~25% of LPS-stimulated genes were downregulated in KO macrophages. In agreement with the limited inhibition, KO macrophages generated by LysM-Cre also showed partial inhibition (13%) of LPS-induced transcription (Fig EV3B and C, and qRT–PCR confirmation in Fig EV3D). Thus, BRD4 is dispensable for > 70% of LPS-induced transcription. Since other BET proteins are shown to affect proinflammatory gene expression, we examined expression of BRD2 and BRD3 in Brd4 KO cells (Belkina *et al*, 2013). Immunoblot data in Fig EV3E revealed that these BET proteins are expressed at slightly higher levels in Brd4 KO cells, indicative of a compensatory mechanism. In GO analysis, BRD4-dependent genes (downregulated by Brd4 knockout) and BRD4-independent genes (unaffected by knockout) show enrichment in inflammation and interferon responses among others (Figs 3F and

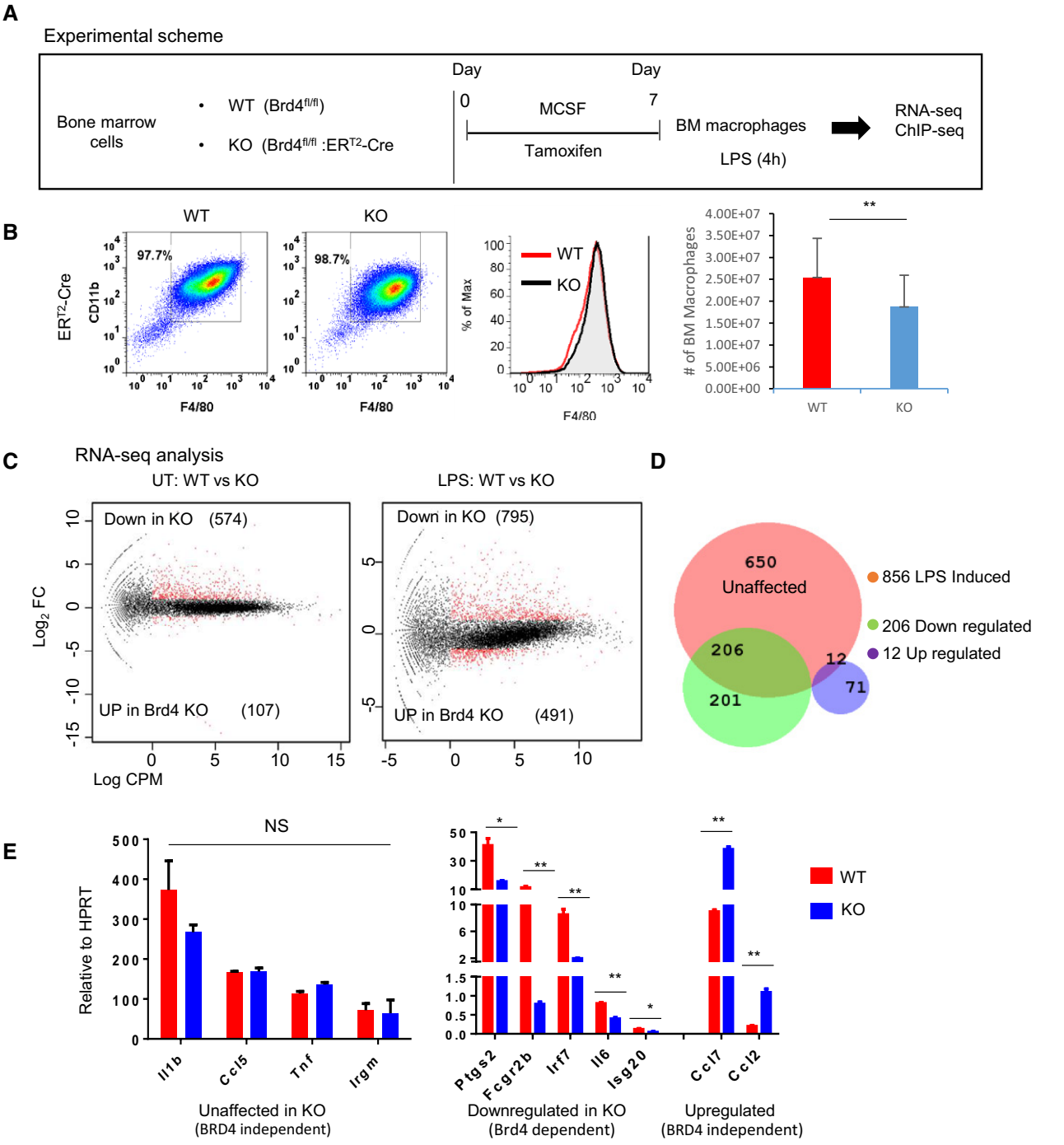

F

Unaffected (BRD4 independent)

GO terms	p-values	overlaps
Acute inflammatory response	1.17E-14	34/148
Type I interferon signaling pathway	6.33E-16	30/148
Positive regulation of NF-kappaB activity	1.49E-14	32/189
TNF-mediated signaling pathway	3.72E-12	35/272
Cellular response to lipopolysaccharide	1.44E-14	27/132
Negative regulation of cell proliferation	3.33E-09	38/399

Downregulated (BRD4 dependent)

GO terms	p-values	overlaps
Inflammatory response	2.882E-07	13/211
Positive regulation of leukocyte migration	2.635E-05	9/151
Activation of MAPK activity	8.582E-05	8/137
Positive regulation of cytokine production	4.927E-05	6/64
Type I interferon signaling pathway	1.47E-04	8/148
Defense response to Gram-positive bacterium	3.48E-04	8/168

Figure 3.

Figure 3. Brd4 deletion partially inhibits LPS-induced gene expression in BM-derived macrophages.

A Experimental scheme for generating BM macrophages. BM cells from Brd4 $^{fl/fl}$ ER^{T2}-Cre mice were cultured in the presence of M-CSF for 7 days and treated with LPS. Brd4 was deleted by tamoxifen treatment (see Fig 1B for verification of Brd4 deletion).

B Flow cytometry profiles of CD11b$^+$ and F4/80$^+$ macrophage population harvested on day 7 from untreated (WT) or tamoxifen-treated (KO) cultures (left). Histogram depicting F4/80 expression levels in WT and KO macrophages (middle). Total number of macrophage yields calculated from > 15 independent experiments. Values represent the average of 21 WT and 24 KO experiments ± SD.

C MA plots of RNA-seq data from untreated (UT) or LPS-treated (4 h) WT and KO macrophages. Differentially expressed genes were identified by a cutoff line of log2 FC > 1 (FDR < 0.1).

D Venn diagram depicting the number of LPS-induced genes in WT and KO macrophages. See explanations in the Figure for overlapped and nonoverlapped genes.

E qRT–PCR analysis of genes representative of the BRD4-independent group (unaffected by KO), BRD4-dependent group (downregulated by KO), or BRD4-independent group (upregulated by KO). Data were obtained from three independent macrophage samples. Values are the average of 3 ± SD.

F GO terms of BRD4-dependent and BRD4-independent genes, analyzed by the Enrichr program. Values in the overlap columns indicate the number of genes found in this study vs total number of genes in the GO terms.

EV3F). Finally, we compared the effect of Brd4 KO and BET inhibitor as reported earlier (Nicodeme *et al*, 2010), and found that 25% of BRD4-dependent genes identified here were shown downregulated by the drug (Appendix Fig S3B). These results indicate that Brd4 KO and BET inhibitors inhibit LPS-stimulated transcription in part through different mechanisms.

LPS treatment increases genome-wide BRD4 occupancy

BRD4 has been shown to bind to broad genomic regions in various cell types (Zhang *et al*, 2012; Lovén *et al*, 2013; Brown Jonathan *et al*, 2014; Kanno *et al*, 2014). In light of a mild inhibition of LPS-induced transcription in KO macrophages, it was important to examine occupancy of BRD4 in macrophages. ChIP-seq analysis for BRD4 revealed ~18,000 peaks and ~43,000 peaks in untreated and LPS-treated macrophages, respectively (Fig 4A). These peaks were distributed widely over the genic and intergenic regions. More than 60% of BRD4 peaks were found in genic regions, while the rest of BRD4 peaks (~40%) were distributed over the intergenic regions (Fig 4A). As depicted in the heat maps in Fig 4B, 4 h of LPS stimulation markedly increased BRD4 signal intensity over the genic regions. Motif analysis identified several transcription factor binding sites near the BRD4 occupied area, including PU.1, AP1, IRFs both in untreated and in LPS-treated macrophages. In addition, the NF-κB site is found near the BRD4 sites after LPS stimulation (Fig 4C). LPS-induced increase in BRD4 signal intensity was presumably due to increased binding of existing BRD4, since BRD4 expression levels did not change after LPS stimulation (Fig 4D). To investigate whether BRD4 binding correlates with BRD4-regulated transcription, we examined average BRD4 occupancy on BRD4-dependent and BRD4-independent genes. LPS stimulation caused a large increase in BRD4 binding both in dependent and in independent genes, showing a peak at the TSS (Fig 4E). Subsequently, binding of RNA polymerase II (Pol II) was increased after LPS treatment, the increase was less in KO cells than WT cells for BRD4-dependent genes (see arrows in Fig 4E). Further, histone modification marks, H3K27ac, H3K9ac, H4tet-ac, H3K4me3, denoting active transcription were increased after LPS stimulation (Figs 4E and EV4A). Gene tracks in Fig 4F show BRD4 ChIP-seq peaks for BRD4-independent and BRD4-dependent genes (Ccl9 and Fcgr2b, respectively), along with Pol II peaks and histone marks. Also aligned are RNA-seq peaks for these genes (see examples of additional gene tracks in Fig EV4B). Although we observed similar results in separate ChIP-seq experiments, inclusion of spike-in controls would have provided more reliable estimates for ChIP signals. To ascertain whether our results, obtained without spike-in controls, are still valid, we performed PCR-based ChIP using macrophage chromatin mixed with *Drosophila* spike-in reagents. Results in Fig EV4C showed a significant reduction in Pol II binding in Brd4 KO cells when tested for BRD4-dependent genes, and no reduction in Pol II binding in BRD4-independent genes. However, BRD4 occupancy was reduced in all genes in KO cells. These results support our point that Pol II occupancy is reduced in KO macrophages for BRD4-dependent genes, but not for BRD4-independent genes.

Together, BRD4 is globally recruited to LPS-stimulated genes, irrespective of whether it is required for transcription. These results indicate that occupancy itself does not imply functional necessity.

LPS stimulation triggers reorganization of super-enhancers

While most enhancers are so-called typical enhancers (TEs), super-enhancers (SEs) are longer in length, encompassing more than 12 Kb, enriched with transcription factors, Pol II, chromatin modifiers, etc. (Hnisz *et al*, 2015, 2017). SEs drive strong transcription from neighboring genes. BRD4 has been identified as a major SE component in leukemia and other cells (Hnisz *et al*, 2013; Lovén *et al*, 2013; Whyte Warren *et al*, 2013). To detect SEs in macrophages, BRD4 ChIP-seq data were analyzed by the SE programs available at: http://younglab.wi.mit.edu/super_enhancer_code.html (Lovén *et al*, 2013; Whyte Warren *et al*, 2013). In the enhancer plots of Fig 5A, DNA elements were arranged according to increasing BRD4 signal intensity in the X- and Y-axes, where SEs are on the right vertical line. We found 266 and 296 SEs in untreated and LPS-treated macrophages, respectively, thus comprising < 7% of total enhancers; however, they were larger in size, carrying higher BRD4 signal intensity than TEs (Fig EV5A and C). These SEs displayed clusters of strong BRD4 peaks over > 12 kb DNA stretch, which coincided with strong Pol II and H3K27ac clusters, fulfilling the SE designation (Fig EV5B; Lovén *et al*, 2013). To ascertain a close relation between BRD4 SEs and those with H3K27ac and Pol II, we examined genes neighboring each of the SEs among those with RPKM > 10 after LPS treatment. Data in Fig EV5D found that 52% of H3K27ac SE and 41% of Pol II SE were shared with BRD4 SEs. It was interesting to note that SEs in untreated and LPS-treated macrophages were distinct, neighboring largely different sets of gene loci (Venn diagram, Fig 5A, right). Accordingly, gene loci neighbored by SEs of untreated and LPS-treated macrophages were associated with somewhat distinct functions (See GO analysis in Appendix Fig S4A). Together, LPS stimulation triggered a large-scale SE reorganization. Thus, LPS-treated macrophages gained 230 new SEs, while losing 82

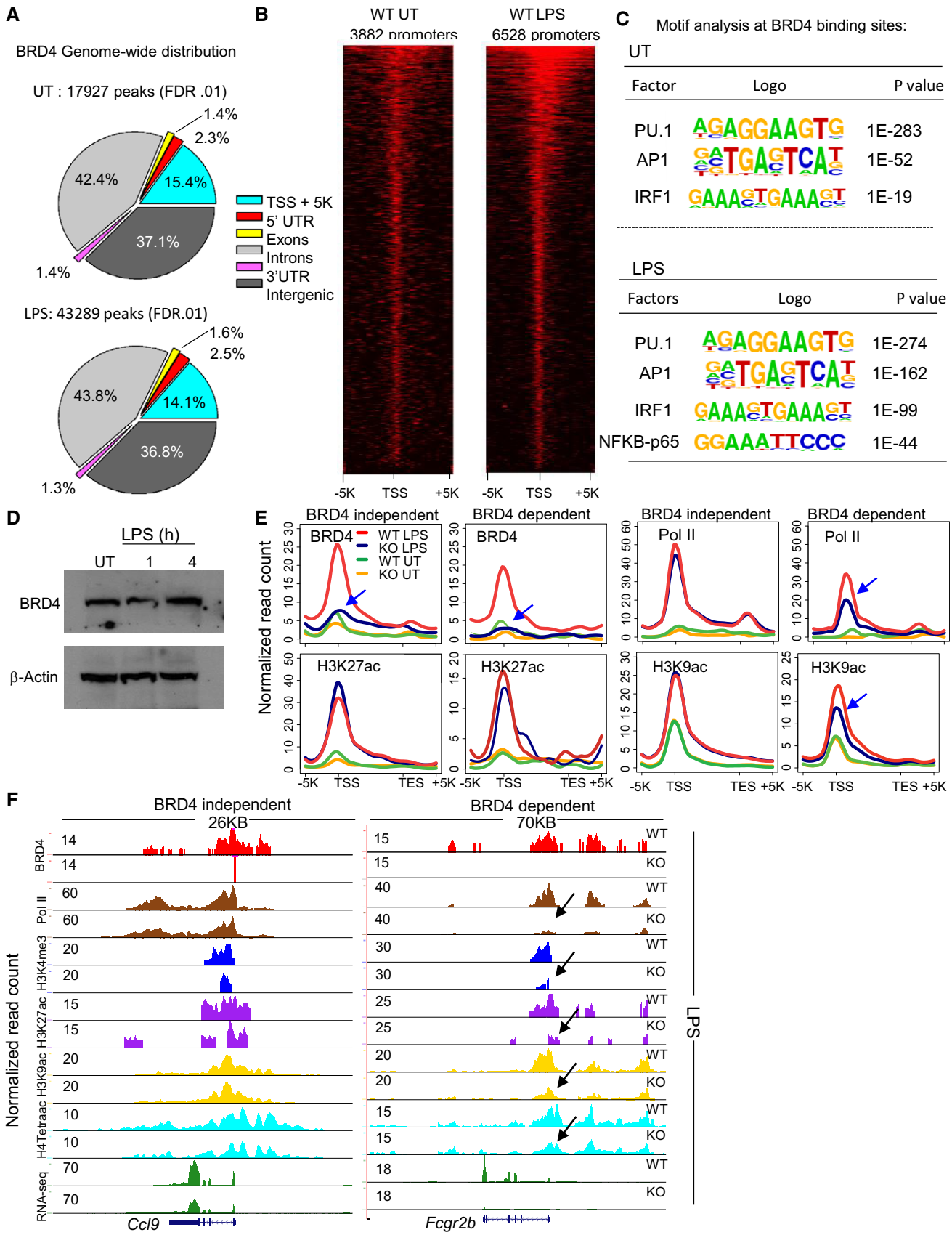

Figure 4.

Figure 4. LPS treatment increases BRD4 binding on BRD4-dependent and BRD4-independent genes.

A Genome-wide distribution of BRD4 in untreated (UT) and LPS-treated macrophages. The numbers on the top represent total peak numbers.
B Heat maps of BRD4 occupancy on the promoter region (TSS ± 5 kb), aligned by the degree of BRD4 signal intensity in UT and LPS-treated macrophages.
C Motif analysis of genome-wide BRD4 binding sites, assessed by the HOMER motif analysis algorithm.
D Immunoblot detection of BRD4 protein levels in UT and LPS-treated WT macrophages. Forty micrograms of whole cell extracts from UT or LPS-treated (1 h or 4 h) macrophages using antibody for BRD4 or β-actin (loading control).
E Binding of BRD4 and Pol II and distribution of histone marks (H3K27ac and H3K9ac) on BRD4-dependent and BRD4-independent genes (from −5 kb of TSS to +5 kb of transcription end site (TES)) in UT and LPS-treated WT and KO macrophages. Normalized ChIP-seq signals (rpm/bp) are shown on the *Y*-axis. Arrows show reduced signals in Brd4 KO macrophages.
F Gene tracks of normalized island-filtered ChIP-seq peaks for BRD4 and Pol II, and indicated histone modification marks, along with RNA-seq peaks for a BRD4-independent gene (*Ccl9*) and a BRD4-dependent gene (*Fcgr2b*). Values on the *Y*-axis are normalized ChIP-seq signals (rpm/bp).

SEs (Fig 5B). Figure 5C presents gene tracks for BRD4 SEs gained or lost after LPS stimulation, illustrating concomitant gain and loss of Pol II and H3K27ac peaks. These results underscore the magnitude and rapidity of SE reorganization, which would lead to extensive transcriptional reprogramming after LPS signaling.

Brd4KO macrophages form alternative super-enhancers

A critical question was whether BRD4 is required for SE formation, as implied by BET inhibitor studies (Lovén *et al*, 2013; Pelish *et al*, 2015). We addressed this question by testing KO macrophages for SEs ranked by Pol II and H3K27ac, authentic SE constituents (Hnisz *et al*, 2013; Whyte Warren *et al*, 2013). Meta-gene alignments in Fig 5D revealed that KO macrophages possessed SEs containing Pol II and H3K27ac, although lacking BRD4. Enhancer plots generated by the H3K27ac ranking showed 381 and 327 SEs in WT and Brd4KO macrophages, respectively (Fig 5E). Importantly, 72% of genes neighbored by the H3K27ac SEs in Brd4 KO cells were common with those in WT macrophages (Venn diagram in Fig 5F, left). Likewise, 67% of SE regions in KO cells overlapped with WT counterparts (Fig 5F right). Motif analysis suggested that shared and unique SEs have a distinct set of transcription factors (Fig EV5E). GO analyses pointed roles in LPS response and inflammation (Appendix Fig S4B). These results indicate that SEs are assembled in KO macrophages without BRD4, and these SEs target a set of genes shared by WT macrophages. These alternative SEs could support a significant fraction of LPS-induced transcription without BRD4.

Increased NF-κB (p65) binding in Brd4KO macrophages

Many LPS-inducible genes are activated by NF-κB(Hargreaves *et al*, 2009). We noticed that some of NF-κB-activated genes were BRD4-independent, e.g., *Il1b*, *Tnf*, and *Ccl5* (see Fig 3E). This raised the possibility that BRD4 is not required for some of NF-κB-dependent transcription. ChIP-seq analysis revealed, surprisingly, that p65 binding was distinctly higher in KO macrophages than in WT macrophages (p65 heat map in Fig 6A). We then examined p65 binding on BRD4-independent and BRD4-dependent genes separately (Fig 6B). Average p65 peak counts were consistently higher in Brd4 KO macrophages than in WT cells when tested for BRD4-independent genes (Fig 6B, top). Moreover, BRD4-dependent genes had virtually no p65 binding. These results suggested that NF-κB binding is a significant factor for defining BRD4 dependence in LPS response. Supporting this notion, NF-κB sites were singled out as the top candidate for BRD4-independent genes as assessed by a TF binding site prediction analysis (Appendix Fig S5A). Gene tracks in Fig 6C show higher p65 binding on *Il1b* and *Ccl7* in Brd4 KO macrophages than WT cells. Conversely, a BRD4-dependent gene, *Ptgs2*, showed very low p65 occupancy in both KO and WT cells (see an additional example in Appendix Fig S5B). We also analyzed ChIP-seq data for p65 binding in enhancer regions and found that KO macrophages had greater p65 occupancy than WT cells (Fig 6D and E). While some of these enhancers were large in length, most of them were < 12 kb and did not appear to meet the definition of SEs. GO analysis pointed p65 enhancers to be associated with genes involved in inflammatory responses (Appendix Fig S5C). Thus, the absence of BRD4 did not reduce LPS-induced NF-κB binding, rather it increased the binding. Immunostaining and immunoblot data suggested that increased NF-κB binding might be due to an increase in p65 access to the cognate sites, rather than increased p65 expression or nuclear residence (Appendix Fig S5D).14 Together, increased NF-κB binding in KO macrophages may provide an additional layer of compensation, allowing KO macrophages to retain significant inflammatory responses.

Discussion

Brd4 deletion in HSCs and macrophages highlighted contrasting roles of BRD4: While Brd4 KO obliterated HSC development, abolishing

Figure 5. Super-enhancers (SEs) in WT and KO macrophages.

A BRD4-bound enhancers within 12.5 kb were stitched together and ranked by BRD4 ChIP-seq signals (rpm) in untreated (UT, left) and LPS-treated (middle) WT macrophages. The dotted line distinguished SEs from TEs. Gene names with the ranking in parenthesis are among genes closest to SEs. Venn diagram (right) showing nearest genes common in UT and LPS-treated macrophages.
B Genome-wide gain and loss of BRD4 SEs upon LPS stimulation. Based on SE coordinates (rpm from LPS-treated samples/rpm in untreated samples), changes greater or less than twofold (log2) were plotted as gain or loss.
C Examples of nearest genes that gained or lost SEs upon LPS treatment. Gene tracks for gained and lost loci (near Tnf and Csf1r) showing clusters of BRD4, Pol II, and H3K27ac signals. Red bar represents SE length.
D Meta-gene alignment of BRD4 signals on BRD4 ranked SEs. Pol II and H3K27ac ChIP-seq reads were aligned centering on BRD4 SEs of LPS-treated WT macrophages.
E Enhancer plots obtained by the H3K27ac ranking in LPS-stimulated WT and KO macrophages.
F Venn diagrams showing genes nearest to H3K27ac SEs common in WT and KO macrophages (left), and H3K27ac SE region from WT and KO macrophages (right).

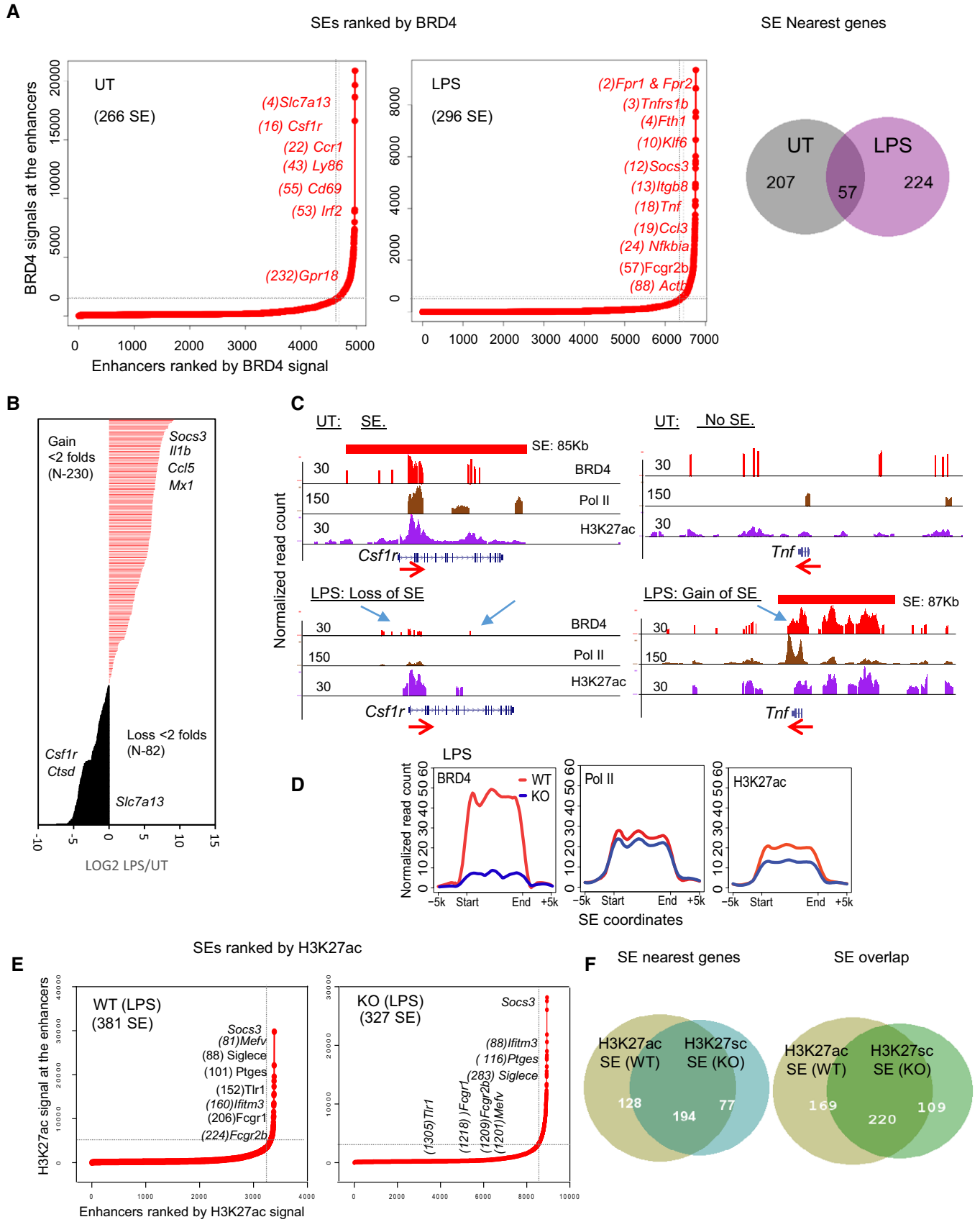

Figure 5.

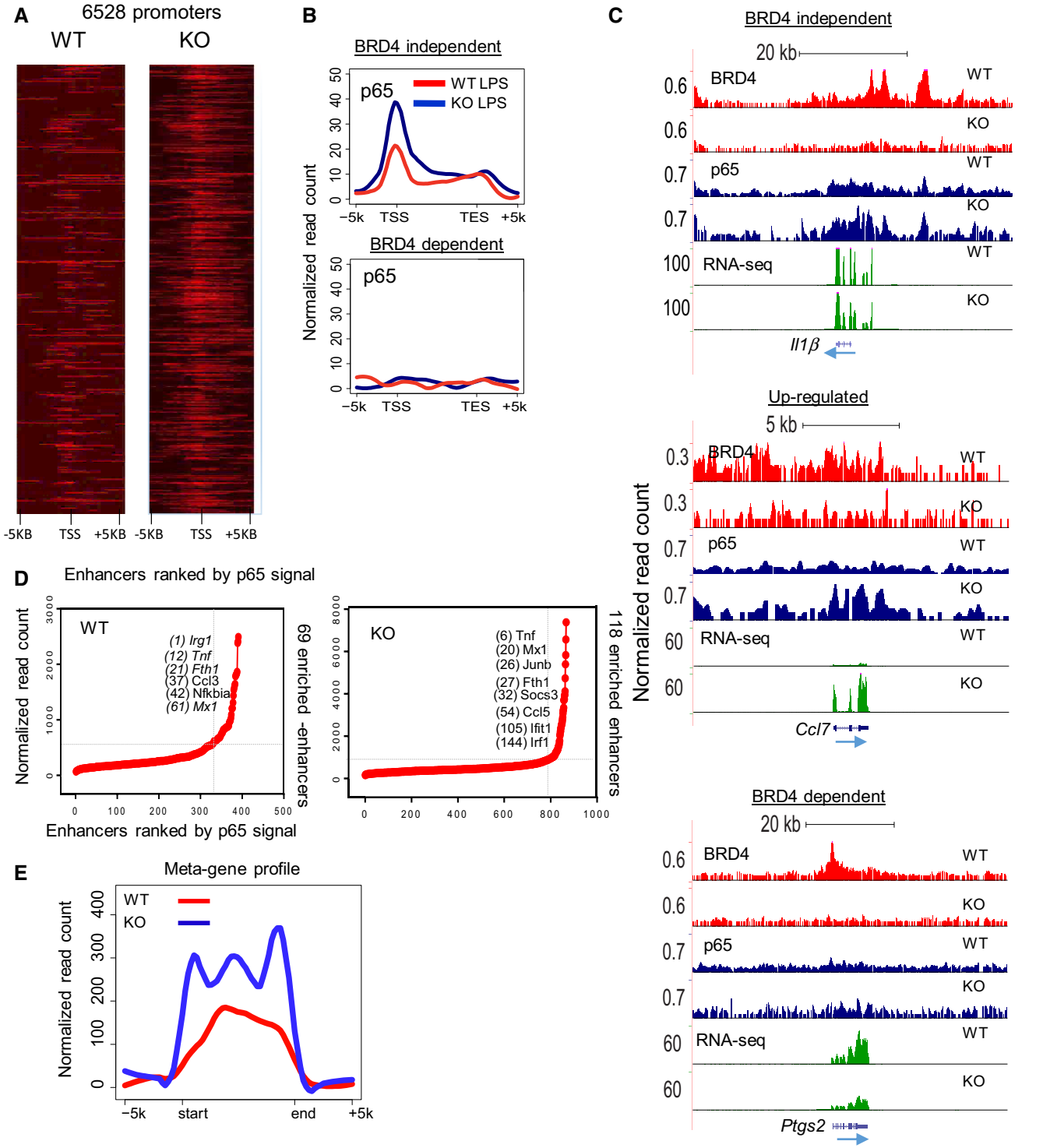

Figure 6. Increased NF-κB binding in Brd4 KO macrophages.

A Heat maps of p65 binding centered at the TSS on BRD4-enriched promoters.

B Meta-gene profile of p65 ChIP-seq signals (rpm/bp) from the TSS to TES and ± 5 kb on BRD4-independent genes (top) and BRD4-dependent genes (bottom).

C Gene tracks of BRD4 and p65 ChIP-seq peaks and RNA-seq profiles on a BRD4-independent gene (*Il1b*), a gene upregulated in Brd4KO macrophages (*Ccl7*), and a BRD4-dependent gene (*Ptgs2*).

D Enhancers ranked by increasing p65 signals in WT (left) and Brd4 KO macrophages (right).

E Meta-gene analysis of p65 occupancy on enhancers in WT (red) and KO macrophages (blue).

the generation of functional immune system, it spared major features of macrophage development, only partially inhibiting LPS responses. The results illustrate context-dependent roles for BRD4. In addition, our study points to a critical requirement of BRD4 for cell proliferation. The developmental defects observed in Brd4 KO HSCs are likely due to their inability to expand as a self-renewing population capable of developing into progenitors. Furthermore, BRD4 was critical for IL-4-induced macrophage proliferation, which was markedly inhibited in Brd4 KO cells. Further supporting the role of BRD4 in cell division, we previously reported that BRD4 knockdown causes reduced fibroblast cell growth, partly due to inhibition of mitotic cycle and G1/S progression (Mochizuki *et al*, 2008; Dey *et al*, 2009). Our results are also in line with the potent cancer growth inhibition reported by BET inhibitors. At the same time, however, our results raise an important possibility that BET inhibitors may adversely affect generation and maintenance of HSCs and other immune cells, which could compromise host defense. With respect to the mechanism, microarray analysis showed inhibition of multiple cell cycle genes including those of mitotic progression in IL-4-treated macrophages. Thus, BRD4 may regulate multiple cell cycle genes in these cells, although it has been proposed that BRD4 drives cancer growth by enhancing c-Myc (Zuber *et al*, 2011; Lovén *et al*, 2013; Pelish *et al*, 2015). Brd4 KO caused modest impairment in macrophage generation and the response to LPS. Given that macrophages are post-mitotic cells (except after IL-4 stimulation), BRD4 may assume a more limited role in nonproliferating cells. In any case, our results underscore extensive redundancy that covers the loss of BRD4, enabling retention of critical macrophage function.

Genome-wide analysis of BRD4 occupancy provided deeper insight into the activity of BRD4 in macrophages. Although KO macrophages suffered relatively minor impairment, suggestive of limited functional involvement, BRD4 broadly occupied the macrophage genome over genic and intergenic regions. In addition, BRD4 binding globally increased after LPS stimulation, both over the genes and over the intergenic enhancers. It is interesting to note that BRD4-independent genes were occupied by BRD4 just as strongly as BRD4-dependent genes. This broad binding underlines a defining feature of BRD4. Namely, BRD4 senses signal-induced changes on histone marks, which sets a stage for global programming of transcriptional paradigm (Kanno *et al*, 2014). Considering that BRD4 would epigenetically influence chromatin landscape, its deletion may impact on a long-term consequence of macrophage activity, although we tested only immediate inflammatory responses in this work.

We present evidence that macrophages possess multiple layers of compensatory mechanisms, which would lessen the impact of BRD4 loss. First, BRD4-independent genes still bound Pol II without BRD4, thus retaining the capacity for transcriptional initiation and elongation. This indicates that there are BRD4-independent mechanisms of transcription. Our data may point to a compensatory role for BRD2 and BRD3, given slightly elevated expression in Brd4 KO cells. It is possible that other factors such as P300/CBP, mediators/adaptors, elongation factors, assembled at the promoter/TSS were sufficient to drive transcriptional initiation and elongation. Second, Brd4 KO macrophages generated SEs containing H3K27ac and Pol II (Hnisz *et al*, 2013; Whyte Warren *et al*, 2013). Remarkably, these SEs targeted many loci that were shared by BRD4 SEs, likely allowing KO macrophages to retain transcription of targeted loci. Together, our results show that BRD4 is not obligatory for SE formation in macrophages, although BRD4 SEs were reported to be critical in cancer cells (Lovén *et al*, 2013; Pelish *et al*, 2015). It is possible that SEs are formed in a nonhierarchical manner, where multiple factors create interactive networks to collectively drive transcription. It should be borne in mind that not all BRD4-containing SEs were rescued in KO macrophages, which may lead to changes in macrophage functions not analyzed in the present study. Lastly, our ChIP-seq data unraveled unexpected enrichment of NF-κB occupancy in Brd4 KO macrophages. NF-κB binding was detected selectively on BRD4-independent genes, but not BRD4-dependent genes. Furthermore, there were more NF-κB-containing enhancers in Brd4 KO macrophages than WT cells. These data suggest that in the absence of BRD4, NF-κB gains increased accessibility to its cognate sites, favoring expression of some NF-κB-dependent inflammatory genes. This compensatory activity may be attributed at least partly to BRD2 and BRD3. Thus, NF-κB expression and nuclear residence were not altered in KO macrophages (Bao *et al*, 2017). Irrespective of the mechanisms, increased NF-κB binding in KO macrophages would provide an added layer of compensation, allowing macrophages to retain their most important role, to mount a timely inflammatory response.

In conclusion, this work shows that BRD4 is essential for the development and execution of immune responses in a context-dependent manner. This work also highlights previously unappreciated compensatory mechanisms that minimize the loss of BRD4 in macrophages. Mechanisms such as this may operate in other post-mitotic cells.

Materials and Methods

Reagents and Tools table

Reagent or Resource	Source	Identifier
Antibodies		
Biotin rat anti-CD3	Biolegend	Cat# 100244, RRID:AB_2563947
Biotin rat anti-CD5	Biolegend	Cat# 100604, RRID:AB_312733
Anti-biotin mouse Alexa 594	Jackson ImmunoResearch	Cat# 200-582-211, RRID:AB_2339043
Biotin hamster anti-CD11c	Biolegend	Cat# 117304, RRID:AB_313773
Biotin hamster anti-TCRγδ	Biolegend	Cat# 118103, RRID:AB_313827

Reagents and Tools table (continued)

Reagent or Resource	Source	Identifier
Biotin rat anti-CD11b	Biolegend	Cat# 101204, RRID:AB_312787
Biotin mouse anti-NK1.1	Biolegend	Cat# 108704, RRID:AB_313391
Biotin rat anti-B220	Biolegend	Cat# 103204, RRID:AB_312989
Biotin rat anti-Ter119	Biolegend	Cat# 116204, RRID:AB_313705
Biotin rat anti-GR1	Biolegend	Cat# 108404, RRID:AB_313369
APC rat anti-cKit	Biolegend	Cat# 105812, RRID:AB_313221
FITC rat anti-SCA1	Biolegend	Cat# 108106, RRID:AB_313343
PE rat anti-FLT3	Biolegend	Cat# 135306, RRID:AB_1877217
PE rat anti-CD71	Biolegend	Cat# 113808, RRID:AB_313569
APC rat anti-TER119	Biolegend	Cat# 116212, RRID:AB_313713
APC rat anti-F4/80	Biolegend	Cat# 123116, RRID:AB_893481
PE rat anti-CD11b	Biolegend	Cat# 101207, RRID: AB_312789
PERCP rat anti-CD11b	Biolegend	Cat# 101230, RRID:AB_2129374
PE rat anti-GR1	Biolegend	Cat# 108408, RRID:AB_313373
FITC rat anti-CD19	Biolegend	Cat# 152404, RRID:AB_2629813
FITC rat anti-B220	Biolegend	Cat# 103206, RRID:AB_312991
FITC mouse anti-BrdU	BD Pharmingen	Cat# 559619, RRID:AB_2617060
FITC mouse anti-Ki-67	BD Pharmingen	Cat# 556026, RRID:AB_396302
FITC mouse anti-arginase	BD Pharmingen	Cat# 610708, RRID:AB_398031
PE rat anti-IgM	Biolegend	Cat# 406508, RRID:AB_315058
Rabbit anti-BRD4	Dey *et al* (2000)	N/A
Rabbit anti-p65	Santa Cruz	Cat# sc-372, RRID:AB_632037
Mouse anti-Pol II	Biolegend	Cat# 904001, RRID:AB_2565036
Rabbit anti-H3K27ac	Abcam	Cat# ab4729, RRID:AB_2118291
Rabbit anti-H3K4me3	Abcam	Cat# ab8580, RRID:AB_306649
Rabbit anti-H3K9ac	EMD Millipore	Cat# 07-352, RRID:AB_310544
Rabbit anti-H4tetra-ac	EMD Millipore	Cat# 06-866, RRID:AB_310270
Mouse anti-β-actin	Cell Signaling	Cat# 3700, RRID:AB_2242334
Mouse anti-α-tubulin	Cell Signaling	Cat# 3873, RRID:AB_1904178
Rat anti-mouse IL-4	BD Biosciences	Cat# 559062, RRID:AB_397187
Rabbit anti-BRD2	Bethyl	Cat# A302-583A, RRID: AB_2034829
Rabbit anti-BRD3	Bethyl	Cat# A302-367A, RRID: AB_1907250
Rabbit anti-TFIIB	Santa Cruz	Cat# sc-271736, RRID:AB_10709889
Spike-in antibody	Active Motif	Cat# 61686, RRID: AB_2737370
Chemicals, peptides, and recombinant proteins		
Murine IL-4	Peprotech	Cat# 214-14
Murine IFN-γ	Peprotech	Cat# 315-05
E. coli LPS	Sigma	Cat# L2018
4-hydroxytamoxifen	Sigma	Cat# H6278
BrdU	BD Pharmingen	Cat# 559619, RRID:AB_2617060
Spike-in chromatin	Active Motif	Cat# 53083
Drosophila-positive control primer set Pbgs	Active Motif	Cat# 71037
Deposited data		
Microarray dataset	This manuscript	GSE104643
RNA sequencing dataset	This manuscript	GSE113009

Reagents and Tools table (continued)

Reagent or Resource	Source	Identifier
ChIP sequencing dataset	This manuscript	GSE113226
Experimental models: organisms/strains		
C57BL/6 Brd4$^{Fl/Fl}$ mice	This manuscript	N/A
B6.Cg-*Commd10*$^{Tg(Vau1\text{-}icre)A2Kio}$/J mice	Jackson	Cat# JAX:008610, RRID:IMSR_JAX:008610
B6.129P2-*Lyz2*$^{tm1(cre)Ifo}$/J	Jackson	Cat# JAX:004781, RRID:IMSR_JAX:004781
B6.Cg-*Ndor1*$^{Tg(UBC\text{-}cre/ERT2)1Ejb}$/1J	Jackson	JAX:007001, RRID:IMSR_JAX:007001
Oligonucleotides		
See Appendix Fig S1A for oligonucleotide sequences		

Methods and Protocols

Mice

All animal protocols were approved by the Animal Care and Use Committee at National Institute of Child Health and Human Development (Animal Study Program #14-044 and #17-044). This guidance ensures a clean, disease-free comfortable living environment for the animals. Brd4 $^{fl/fl}$ mice were constructed by homologous recombination using the ~20 kb targeting vector containing loxP sites flanking exon 3 of the Brd4 locus (Fig 1A). The vector was transfected into murine 129 R1 ES cells. Recombinant ES cells were injected into the blastocysts to generate chimeric mice. Mice with germ line transmission were mated with those carrying the FLP recombinase to remove the neo fragment. Resultant Brd4 $^{fl/+}$ mice were crossed with C57BL/6 mice for at least four generations. The wild-type and recombined alleles were identified by PCR-based genotyping using primers in Appendix Fig S1A. Mice with conditional or wild-type (WT) allele (Brd4 $^{fl/fl}$ or Brd4 $^{fl/+}$, Brd4$^{+/+}$) were crossed with transgenic mice carrying Vav-Cre (The Jackson Laboratory strain 008610), LysM-Cre (The Jackson Laboratory strain 004781), or ER^{T2}-Cre (The Jackson Laboratory strain 007001).

Cell preparations and flow cytometry

Single-cell suspensions were prepared from fetal liver, spleen, bone marrow, and peritoneum. For lineage-specific labeling, fetal liver cells were stained with biotinylated antibodies from Biolegend, against CD3 (17A2), CD5 (53–7.3), CD11c (N418), TCRγδ (UC7-13D5), CD11b (M1/70), NK1.1 (PK136), B220 (RA3-6B2), TER-119, GR1 (RB6-8C5), and anti-biotin Alexa 594 secondary antibody. Other fluorescence-conjugated antibodies used for detection of progenitors and differentiated hematopoietic cells were cKit (2B8), SCA1 (E13-161.7), FLT3 (A2F10), CD16/32 (2.4G2), CD4 (GK1.5), CD8 (53–6.7), CD71 (R-17217), CD19 (6D5), F4/80 (BM8), IgM (RMM-1), CD11b (M1/70) all from Biolegend. For cell proliferation assays, peritoneal cells were fixed, permeabilized, and stained with antibodies against BrdU (BD Pharmingen 51-9000019AK), Ki-67 (BD Bioscience), and ARG1 (BD Bioscience). Stained cells were analyzed by FACSCalibur or LSR II (BD Biosciences). Data were analyzed using FlowJo software (Tree Star). Statistical significance of cell number differences between WT and KO was determined by unpaired t-test using GraphPad software.

Bone marrow (BM)-derived macrophages and LPS treatment

Freshly isolated bone marrow cells were cultured in the presence of F12/DMEM supplemented with 20% L929 conditioned medium containing M-CSF for 7 days. To activate ER^{T2}-Cre, 4 μM of 4-hydroxytamoxifen (Sigma) was added to the culture media starting on day 1. Fresh tamoxifen was supplemented every other day for 6 days. On day 7, macrophages from BRD4 $^{fl/fl}$ ER^{T2}-Cre and control mice were treated with 100 ng/ml LPS (*E. Coli*, Sigma) for 4 h. Peritoneal macrophages from BRD4 $^{fl/fl}$ LysM-Cre and control mice were injected with IL-4C through i.p. (Jenkins *et al*, 2011) or treated *ex vivo* with 1 ng/ml IL-4 (Peprotech). To isolate peritoneal macrophages, peritoneal cells were incubated with biotinylated antibodies to CD19 (6D5), CD5 (53–7.3), CD3 (17A2), CD4 (GK1.5), CD8 (53–6.7), NK1.1 (PK136) all from Biolegend and streptavidin-coated microbeads. The mixtures were applied on the MACS separation system to collect the flow-through fraction (Miltenyi).

Microarray and RNA-seq

Total RNA was isolated using RNeasy Kit (Qiagen). Microarray analysis was performed for duplicate samples from each group using the GeneChIP mouse gene 1.0 ST array system (Affymetrix), according to the manufacturer's instruction at EA/Quintiles. Raw data were analyzed using GeneSpring software (Agilent). Raw data files are available at the NCBI Gene Expression Omnibus (GEO) server under the accession number GSE104643.

For RNA-seq, total RNA was prepared using RNeasy Mini Kit (Qiagen), then subjected to oligo-dT selection by using Dynal magnetic beads (Invitrogen) according to the manufacturer's protocol. Resultant mRNA was fragmented by heating at 94°C for 3 min in the fragmentation buffer (40 mM Tris-acetate, pH 8.2, 100 mM potassium acetate, and 30 mM magnesium acetate). RNA fragments were precipitated with GlycoBlue (Ambion), used as a carrier, and reverse-transcribed by SuperScript II reverse transcriptase (Invitrogen) with random primer and RNasin (Promega). Second-strand cDNAs were synthesized using *E. coli* DNA polymerase I and RNaseH (Invitrogen). Purification of second-strand cDNAs was performed with ZYMO DNA Clean & Concentrator-5 Kit. Library preparation, including ligating barcode, was performed using a Mondrian SP (NuGEN Technologies Inc.) and the Ovation SP Ultralow Library system (NuGEN). Fragments ranging from 250 to 450 bp were selected and subjected to paired-end sequencing on a HiSeq 2000 sequencing system (Illumina). For RNA-seq analysis, paired-end reads were aligned to the Mus musculus reference genome mm9 using Burrows-Wheeler Aligner with default

parameters. Uniquely mappable reads were retained for further analysis. Transcript abundance was quantified using rpkm. The edgeR software was then applied to define differentially expressed genes with *P*-values and FDR (Ramskold *et al*, 2009; Robinson *et al*, 2009). Genes showing an expression change in more than twofold were considered differentially expressed. Raw data files are available at the NCBI Gene Expression Omnibus (GEO) server under the accession number GSE113009. GO analysis was performed using the Enrichr program (Chen *et al*, 2013).

Immunoprecipitation and ChIP-seq

Wild-type and KO BM-derived macrophages (~ 5×10^6 in 15-cm plate) were fixed with 1% formaldehyde (Sigma) in buffer A (50 mM HEPES, pH 7.5, 100 mM NaCl, 1 mM EDTA, and 0.5 mM EGTA) for 10 min and quenched with 0.125 M glycine for 5 min. Cells were washed and incubated in nucleus isolation buffer (10 mM HEPES, pH 7.6, 85 mM KCl, 0.5% NP-40). Nuclear pellets (~2×10^7) were re-suspended in 1 ml shearing buffer (1× TE, pH 8, and 0.1% SDS) and transferred to Covaris millitubes and sonicated in Covaris S200 sonicator. Sonicated chromatin was precipitated with antibodies pre-bound to Dynabeads Protein G (Thermo Fisher). Antibodies used were as follows: Brd4 (Dey *et al*, 2000), p65 (Santa Cruz, Cat# sc-372), Pol II (Biolegend, CTD4H8), H3K4me3 (Abcam, ab8580), H3K27ac (Abcam, ab4729), H3K9ac (EMD Millipore 07-352), H4tetra-ac (EMD Millipore 06-866). Immunoprecipitated DNA was de-crosslinked, digested with proteinase K, and purified using QIAquick PCR Purification Kit (Qiagen). Precipitated DNA was used for validation by qChIP. Twenty to 50 ng of precipitated DNA was used for library construction using Ovation Ultralow Library System V2 (NuGEN). Briefly, ChIP DNA was processed stepwise in the automated hand-free system workstation starting with sample concentration using Agencourt RNA Clean XP Purification Beads, end repair, adaptor ligation, and a final purification of samples. Libraries were processed immediately and enriched by 10–12 cycles of PCR amplification. Library DNA was gel-fractionated, purified, quantified using Bioanalyzer. Library DNA with fragment length of 200-400 bp was subjected to single-end sequencing on a HiSeq 2000 sequencing system (Illumina).

Spike-in normalization in PCR-ChIP

Sonicated chromatin from ~5×10^5 LPS-treated macrophages was mixed with 20 ng of spike-in Drosophila chromatin (Active Motif), incubated with antibody for mouse chromatin along with 2 μg of spike-in control antibody (Active Motif), and then precipitated with Protein G Dynabeads (Thermo Fisher). Immunoprecipitated DNA was amplified using primers for the TSS area of indicated mouse genes and the Drosophila primer set (Active Motif). C_t values obtained from Drosophila primer set were used to normalize ChIP data for each antibody.

ChIP-seq data analysis

ChIP-seq reads were aligned to the mouse reference genome (mm9) using BWA (Li & Durbin, 2009) with default parameters. Uniquely mapped reads were retained for downstream analysis. Peak calling was performed using SICER (Zang *et al*, 2009). Accordingly, for BRD4, a window and gap were set at 50 bp with 0.01 FDR. For other ChIP-seq, peak calling, window, and gap were at 200 bp with FDR at 0.01. Raw data files are available at the NCBI Gene Expression Omnibus (GEO) server under the accession number GSE113226. Data from immunoprecipitated samples were normalized to those with input DNA. UCSC genome tracks were generated using SICER wiggle outputs and were uploaded and viewed at http://genome.ucsc.edu. Chip-seq data were analyzed by the following means. *Meta-gene profile:* To create a meta-gene profile for ChIP-seq binding, density of BRD4, Pol II, p65, H3K4me3, H3K27ac, H3K9ac, and H4tetra-ac that was determined by binning the TSS to TES region into 10 bins plus 5 kb upstream of TSS and 5 kb downstream of TES was plotted at 50-bp resolution. Density of ChIP-seq signals was determined for these three regions by averaging rpm/bp and was plotted as unit of normalized read count (Figs 4E, 6B and EV4A). *Heat maps for BRD4 occupancy:* To generate heat maps for BRD4 occupancy on promoters, BRD4 signals were displayed on the promoter regions (encompassing the TSS and ± 5 kb), from untreated and LPS-treated macrophages (~4,000 and ~6,500, respectively; Fig 4B). Rows are ranked by BRD4 signal intensity. *Identification of super-enhancers (SEs):* We identified super-enhancers using the ROSE algorithm available at http://younglab.wi.mit.edu/super_enhancer_code.html (Lovén *et al*, 2013; Whyte Warren *et al*, 2013). We used the default parameters for stitching together peaks that were within 12.5 kb with an TSS exclusion zone of 2.5 kb. Background-subtracted stitched ChIP-seq peaks (rpm) and their counterpart of unstitched peaks were plotted with increasing intensities on the *X*-axis. The enrichment intensities of those that were above the inflection point were called super-enhancers (Fig 5A and E). Gain and loss of BRD4 SEs were determined by at least twofold changes in BRD4 signals in one or the other direction (Fig 5B). *Meta-gene representation of BRD4 SEs*: BRD4 distribution was determined by binning enhancers into three regions: (i) SE regions were divided into 10 bins, regardless of the size, (ii) 5 kb upstream from the start, and 3) 5 kb downstream from the end. This allowed SEs of all sizes to align at a fixed start and stop sites. The average of normalized read count of ChIP-seq signals was plotted on the *Y*-axis (Fig 5D). ChIP-seq signals by Pol II and H3K27ac were aligned on BRD4-enriched SE coordinates. Enhancers with high p65 signals were identified based on a similar method as above, although most of p65 enhancers were < 12.5 kb in length (Fig 6D).

Statistical analysis

Statistical significance of the differences in gene expression and differences in hematopoietic cell population between WT and KO was determined by two-tailed *t*-test using GraphPad Prism QuickCalcs software. A *P*-value of < 0.05 was considered significant. Data are presented as means ± SD and are clearly indicated in figure legends.

Data availability

Microarray, RNA-seq and ChIP-seq data are available at https://www.ncbi.nlm.nih.gov/geo/query/acc.cgi and are under accession number GSE104643, GSE113009 and GSE113226 respectively.

Expanded View for this article is available online.

Acknowledgements

The authors are indebted to late Dr. W. Paul (NIAID) for discussion of this project and his suggestion on IL-4C experiments. We thank T. Myers (NIAID)

for initial help with microarray analyses, JE. Lee and K. Ge (NIDDK) for reagents, M. Bachu for suggestion with ChIP-seq data analysis and NCI FACS core facility. We thank Matsuyama (Tokyo Japan), J. Kassis, and P. Love (NICHD) for discussion. This research was supported by the Intramural Research Program of NICHD, NIH.

Author contributions

KO and AD conceived the study and wrote the paper. AN and AlG generated $Brd4^{Fl/Fl}$ mice. AD, AnG, and RY performed all experiments. WY and RP performed bioinformatics analyses for RNA-seq and ChIP-seq data. FDF contributed to critical methodology. KP, JiZ, DS, and JuZ provided conceptual insights and experimental design.

Conflict of interest

The authors declare that they have no conflict of interest.

References

Adolfsson J, Månsson R, Buza-Vidas N, Hultquist A, Liuba K, Jensen CT, Bryder D, Yang L, Borge O-J, Thoren LAM, Anderson K, Sitnicka E, Sasaki Y, Sigvardsson M, Jacobsen SEW (2005) Identification of Flt3 + Lympho-myeloid stem cells lacking erythro-megakaryocytic potential: a revised road map for adult blood lineage commitment. *Cell* 121: 295 – 306

Anand P, Brown Jonathan D, Lin Charles Y, Qi J, Zhang R, Artero Pedro C, Alaiti MA, Bullard J, Alazem K, Margulies Kenneth B, Cappola Thomas P, Lemieux M, Plutzky J, Bradner James E, Haldar Saptarsi M (2013) BET bromodomains mediate transcriptional pause release in heart failure. *Cell* 154: 569 – 582

Andrieu G, Belkina AC, Denis GV (2016) Clinical trials for BET inhibitors run ahead of the science. *Drug Discov Today Technol* 19: 45 – 50

Bandukwala HS, Gagnon J, Togher S, Greenbaum JA, Lamperti ED, Parr NJ, Molesworth AMH, Smithers N, Lee K, Witherington J, Tough DF, Prinjha RK, Peters B, Rao A (2012) Selective inhibition of $CD4^+$ T-cell cytokine production and autoimmunity by BET protein and c-Myc inhibitors. *Proc Natl Acad Sci* 109: 14532 – 14537

Bao Y, Wu X, Chen J, Hu X, Zeng F, Cheng J, Jin H, Lin X, Chen L-F (2017) Brd4 modulates the innate immune response through Mnk2–eIF4E pathway-dependent translational control of IκBα. *Proc Natl Acad Sci* 114: E3993 – E4001

Belkina AC, Denis GV (2012) BET domain co-regulators in obesity, inflammation and cancer. *Nat Rev Cancer* 12: 465 – 477

Belkina AC, Nikolajczyk BS, Denis GV (2013) BET protein function is required for inflammation: Brd2 genetic disruption and BET inhibitor JQ1 impair mouse macrophage inflammatory responses. *J Immunol* 190: 3670 – 3678

Berthon C, Raffoux E, Thomas X, Vey N, Gomez-Roca C, Yee K, Taussig DC, Rezai K, Roumier C, Herait P, Kahatt C, Quesnel B, Michallet M, Recher C, Lokiec F, Preudhomme C, Dombret H (2016) Bromodomain inhibitor OTX015 in patients with acute leukaemia: a dose-escalation, phase 1 study. *Lancet Haematol* 3: e186 – e195

Bhagwat Anand S, Roe J-S, Mok Beverly YL, Hohmann Anja F, Shi J, Vakoc Christopher R (2016) BET bromodomain inhibition releases the mediator complex from select cis-regulatory elements. *Cell Rep* 15: 519 – 530

Brown Jonathan D, Lin Charles Y, Duan Q, Griffin G, Federation AJ, Paranal Ronald M, Bair S, Newton G, Lichtman AH, Kung AL, Yang T, Wang H, Luscinskas Francis W, Croce KJ, Bradner James E, Plutzky J (2014) NF-κB directs dynamic super enhancer formation in inflammation and atherogenesis. *Mol Cell* 56: 219 – 231

Ceribelli M, Kelly PN, Shaffer AL, Wright GW, Xiao W, Yang Y, Mathews Griner LA, Guha R, Shinn P, Keller JM, Liu D, Patel PR, Ferrer M, Joshi S, Nerle S, Sandy P, Normant E, Thomas CJ, Staudt LM (2014) Blockade of oncogenic IκB kinase activity in diffuse large B-cell lymphoma by bromodomain and extraterminal domain protein inhibitors. *Proc Natl Acad Sci* 111: 11365 – 11370

Chen EY, Tan CM, Kou Y, Duan Q, Wang Z, Meirelles GV, Clark NR, Ma'ayan A (2013) Enrichr: interactive and collaborative HTML5 gene list enrichment analysis tool. *BMC Bioinformatics* 14: 128

Devaiah BN, Case-Borden C, Gegonne A, Hsu CH, Chen Q, Meerzaman D, Dey A, Ozato K, Singer DS (2016) BRD4 is a histone acetyltransferase that evicts nucleosomes from chromatin. *Nat Struct Mol Biol* 23: 540 – 548

Dey A, Ellenberg J, Farina A, Coleman AE, Maruyama T, Sciortino S, Lippincott-Schwartz J, Ozato K (2000) A bromodomain protein, MCAP, associates with mitotic chromosomes and affects G2-to-M transition. *Mol Cell Biol* 20: 6537 – 6549

Dey A, Chitsaz F, Abbasi A, Misteli T, Ozato K (2003) The double bromodomain protein Brd4 binds to acetylated chromatin during interphase and mitosis. *Proc Natl Acad Sci* 100: 8758 – 8763

Dey A, Nishiyama A, Karpova T, McNally J, Ozato K (2009) Brd4 marks select genes on mitotic chromatin and directs postmitotic transcription. *Mol Biol Cell* 20: 4899 – 4909

Duan Q, McMahon S, Anand P, Shah H, Thomas S, Salunga HT, Huang Y, Zhang R, Sahadevan A, Lemieux ME, Brown JD, Srivastava D, Bradner JE, McKinsey TA, Haldar SM (2017) BET bromodomain inhibition suppresses innate inflammatory and profibrotic transcriptional networks in heart failure. *Sci Transl Med* 9: eaah5084

Filippakopoulos P, Qi J, Picaud S, Shen Y, Smith WB, Fedorov O (2010) Selective inhibition of BET bromodomains. *Nature* 468: 1067 – 1073

Fu W, Farache J, Clardy SM, Hattori K, Mander P, Lee K, Rioja I, Weissleder R, Prinjha RK, Benoist C, Mathis D (2014) Epigenetic modulation of type-1 diabetes via a dual effect on pancreatic macrophages and β cells. *eLife* 3: e04631

Georgiades P, Ogilvy S, Duval H, Licence DR, Charnock-Jones DS, Smith SK, Print CG (2002) vavCre Transgenic mice: a tool for mutagenesis in hematopoietic and endothelial lineages. *Genesis* 34: 251 – 256

Ghosh GC, Bhadra R, Ghosh RK, Banerjee K, Gupta A (2017) RVX 208: a novel BET protein inhibitor, role as an inducer of apo A-I/HDL and beyond. *Cardiovasc Ther* 35: e12265

Ghosn EEB, Cassado AA, Govoni GR, Fukuhara T, Yang Y, Monack DM, Bortoluci KR, Almeida SR, Herzenberg LA, Herzenberg LA (2010) Two physically, functionally, and developmentally distinct peritoneal macrophage subsets. *Proc Natl Acad Sci USA* 107: 2568 – 2573

Hargreaves DC, Horng T, Medzhitov R (2009) Control of inducible gene expression by signal-dependent transcriptional elongation. *Cell* 138: 129 – 145

Hnisz D, Abraham Brian J, Lee Tong I, Lau A, Saint-André V, Sigova Alla A, Hoke Heather A, Young Richard A (2013) Super-enhancers in the control of cell identity and disease. *Cell* 155: 934 – 947

Hnisz D, Schuijers J, Lin Charles Y, Weintraub Abraham S, Abraham Brian J, Lee Tong I, Bradner James E, Young Richard A (2015) Convergence of developmental and oncogenic signaling pathways at transcriptional super-enhancers. *Mol Cell* 58: 362 – 370

Hnisz D, Shrinivas K, Young RA, Chakraborty AK, Sharp PA (2017) A phase separation model predicts key features of transcriptional control. *Cell* 169: 13 – 23

Jang MK, Mochizuki K, Zhou M, Jeong H-S, Brady JN, Ozato K (2005) The bromodomain protein Brd4 is a positive regulatory component of P-TEFb and stimulates RNA polymerase II-dependent transcription. *Mol Cell* 19: 523 – 534

Jenkins SJ, Ruckerl D, Cook PC, Jones LH, Finkelman FD, van Rooijen N, MacDonald AS, Allen JE (2011) Local macrophage proliferation, rather than

recruitment from the blood, is a signature of TH2 inflammation. *Science* 332: 1284

Jenkins SJ, Ruckerl D, Thomas GD, Hewitson JP, Duncan S, Brombacher F, Maizels RM, Hume DA, Allen JE (2013) IL-4 directly signals tissue-resident macrophages to proliferate beyond homeostatic levels controlled by CSF-1. *J Exp Med* 210: 2477 – 2491

Kanno T, Kanno Y, LeRoy G, Campos E, Sun H-W, Brooks SR, Vahedi G, Heightman TD, Garcia BA, Reinberg D, Siebenlist U, O'Shea JJ, Ozato K (2014) BRD4 assists elongation of both coding and enhancer RNAs by interacting with acetylated histones. *Nat Struct Mol Biol* 21: 1047 – 1057

Li H, Durbin R (2009) Fast and accurate short read alignment with Burrows-Wheeler transform. *Bioinformatics* 25: 1754 – 1760

Lovén J, Hoke Heather A, Lin Charles Y, Lau A, Orlando David A, Vakoc Christopher R, Bradner James E, Lee Tong I, Young Richard A (2013) Selective inhibition of tumor oncogenes by disruption of super-enhancers. *Cell* 153: 320 – 334

Mele DA, Salmeron A, Ghosh S, Huang H-R, Bryant BM, Lora JM (2013) BET bromodomain inhibition suppresses TH17-mediated pathology. *J Exp Med* 210: 2181 – 2190

Mochizuki K, Nishiyama A, Jang MK, Dey A, Ghosh A, Tamura T, Natsume H, Yao H, Ozato K (2008) The bromodomain protein Brd4 stimulates G1 gene transcription and promotes progression to S Phase. *J Biol Chem* 283: 9040 – 9048

Nicodeme E, Jeffrey KL, Schaefer U, Beinke S, Dewell S, Chung C-W, Chandwani R, Marazzi I, Wilson P, Coste H, White J, Kirilovsky J, Rice CM, Lora JM, Prinjha RK, Lee K, Tarakhovsky A (2010) Suppression of inflammation by a synthetic histone mimic. *Nature* 468: 1119 – 1123

Nishiyama A, Dey A, Miyazaki J-I, Ozato K (2006) Brd4 is required for recovery from antimicrotubule drug-induced mitotic arrest: preservation of acetylated chromatin. *Mol Biol Cell* 17: 814 – 823

Pelish HE, Liau BB, Nitulescu II, Tangpeerachaikul A, Poss ZC, Da Silva DH, Caruso BT, Arefolov A, Fadeyi O, Christie AL, Du K, Banka D, Schneider EV, Jestel A, Zou G, Si C, Ebmeier CC, Bronson RT, Krivtsov AV, Myers AG *et al* (2015) Mediator kinase inhibition further activates super-enhancer-associated genes in AML. *Nature* 526: 273

Ramskold D, Wang ET, Burge CB, Sandberg R (2009) An abundance of ubiquitously expressed genes revealed by tissue transcriptome sequence data. *PLoS Comput Biol* 5: e1000598

Robinson MD, McCarthy DJ, Smyth GK (2009) edgeR: a Bioconductor package for differential expression analysis of digital gene expression data. *Bioinformatics* 26: 139 – 140

Whyte Warren A, Orlando David A, Hnisz D, Abraham Brian J, Lin Charles Y, Kagey Michael H, Rahl Peter B, Lee Tong I, Young Richard A (2013) Master transcription factors and mediator establish super-enhancers at key cell identity genes. *Cell* 153: 307 – 319

Winter GE, Mayer A, Buckley DL, Erb MA, Roderick JE, Vittori S, Reyes JM, di Iulio J, Souza A, Ott CJ, Roberts JM, Zeid R, Scott TG, Paulk J, Lachance K, Olson CM, Dastjerdi S, Bauer S, Lin CY, Gray NS *et al* (2017) BET bromodomain proteins function as master transcription elongation factors independent of CDK9 recruitment. *Mol Cell* 67: 5 – 18.e19

Wu C, Ghosh S (2003) Differential phosphorylation of the signal-responsive domain of I kappa B alpha and I kappa B beta by I kappa B kinases. *J Biol Chem* 278: 31980 – 31987

Yang Z, Yik JHN, Chen R, He N, Jang MK, Ozato K, Zhou Q (2005) Recruitment of P-TEFb for stimulation of transcriptional elongation by the bromodomain Protein Brd4. *Mol Cell* 19: 535 – 545

Zang C, Schones DE, Zeng C, Cui K, Zhao K, Peng W (2009) A clustering approach for identification of enriched domains from histone modification ChIP-Seq data. *Bioinformatics* 25: 1952 – 1958

Zhang W, Prakash C, Sum C, Gong Y, Li Y, Kwok JJT, Thiessen N, Pettersson S, Jones SJM, Knapp S, Yang H, Chin K-C (2012) Bromodomain-containing Protein 4 (BRD4) regulates RNA polymerase II serine 2 Phosphorylation in human $CD4^+$ T Cells. *J Biol Chem* 287: 43137 – 43155

Zuber J, Shi J, Wang E, Rappaport AR, Herrmann H, Sison EA, Magoon D, Qi J, Blatt K, Wunderlich M, Taylor MJ, Johns C, Chicas A, Mulloy JC, Kogan SC, Brown P, Valent P, Bradner JE, Lowe SW, Vakoc CR (2011) RNAi screen identifies Brd4 as a therapeutic target in acute myeloid leukaemia. *Nature* 478: 524